Dynamics of tidal mixing fronts in the North Sea

By A. E. Hill[1], I. D. James[2], P. F. Linden[3], J. P. Matthews[1], D. Prandle[2], J. H. Simpson[1], E. M. Gmitrowicz[4,5], D. A. Smeed[3,6], K. M. M. Lwiza[1,7], R. Durazo[1], A. D. Fox[1,8] and D. G. Bowers[1]

[1] *School of Ocean Sciences, University of Wales Bangor, Marine Science Laboratories, Menai Bridge, Gwynedd LL59 5EY, U.K.*

[2] *Proudman Oceanographic Laboratory, Bidston Observatory, Birkenhead L43 7RA, U.K.*

[3] *Department of Applied Mathematics and Theoretical Physics, University of Cambridge, Silver Street, Cambridge CB3 9EW, U.K.*

[4] *Ministry of Agriculture Fisheries and Food, Directorate of Fisheries Research, Fisheries Laboratory, Lowestoft, Suffolk NR33 0HT, U.K.*

Twenty years since the discovery of tidal mixing fronts there are still few convincing observations of the velocity field associated with these structures. Simple models of shelf sea fronts predict strong along-front jets, weaker convergent circulations and instabilities. During the North Sea Project a series of studies of the Flamborough frontal system has used a new approach based upon novel combinations of modern instrumentation (HF radar, acoustic Doppler current profiler, Decca-Argos drifting buoys and towed undulating CTD) and have provided one of the first directly observed pictures of shelf sea frontal circulation. Observational confirmation of jet-like along-front flow has been found together with evidence of cross-frontal convergence. A new generation of eddy-resolving models will help to focus the next phase of frontal circulation studies in relation to questions concerning baroclinic instability and eddy generation.

1. Introduction

Tidal mixing fronts form the boundary between vertically mixed and summer-stratified waters in shelf seas. Since their discovery, they have been the focus of considerable attention for their potential role as sites of enhanced primary and secondary biomass production (reviewed by Le Fèvre (1986)) and extensive accounts of them have appeared in textbooks. However, in some respects, our understanding of tidal frontal systems has moved on very little since the time of their discovery.

Frontal physics has been concerned firstly with observations and modelling designed to understand the location and seasonal evolution of fronts (Simpson 1981; Soulsby 1983) and secondly with model development to predict the flows generated by frontal density gradients (James 1978, 1990; Garrett & Loder 1981). There are, however, very few observations of the velocity field at fronts against which to test the predictions of the latter class of models. Figure 1 summarizes schematically the

Present addresses: [5] Wallace Evans, Tremains House, Tremains Court, Bridgend CF31 2AR, U.K. [6] James Rennell Centre for Ocean Circulation, Gamma House, Chilworth Research Centre, Southampton S01 7NS, U.K. [7] Marine Sciences Research Center, State University of New York at Stony Brook, Stony Brook, New York 11794–5000, U.S.A. [8] Department of Mathematics, University of Exeter, Exeter EX4 4QE, U.K.

Phil. Trans. R. Soc. Lond. A (1993) **343**, 431–446
Printed in Great Britain

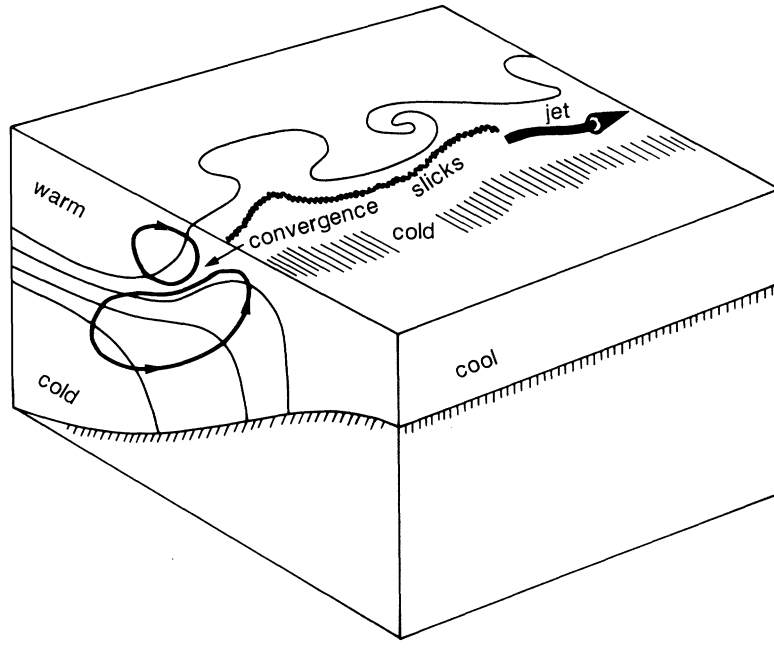

Figure 1. Frontal circulation paradigm showing an along-front jet and two-cell transverse circulation.

present two-dimensional, steady-state paradigm of density-driven circulation at tidal mixing fronts which arises from a combination of observations and model predictions. The most pronounced feature of the circulation is an along-front, near-geostrophic jet driven by the cross-front density-induced pressure gradient. For typical shelf sea density gradients, jet speeds of order 0.15 m s^{-1} are predicted.

Internal friction will retard the along-front jet so that not all of the cross-front pressure gradient is in equilibrium with the Coriolis force. Consequently the unbalanced part of the pressure field is predicted to drive a weak (less than 0.05 m s^{-1}) secondary circulation in the plane perpendicular to the front. Frictionally induced transverse circulation is like a slowed-down form of how the front would collapse under gravity if the geostrophic constraint was removed altogether, although the analogy is imperfect. The transverse circulation implies upwelling of cold, bottom water on the mixed side of the front and is consistent with observed surface temperature minima on the mixed side (Simpson *et al.* 1978) and upward-doming of bottom front isotherms. Secondary circulation also implies surface flow convergence although this is not necessarily located at the point of maximum horizontal density gradient. Surface slicks and accumulation of debris near tidal mixing fronts support the picture of surface convergence.

A steady-state picture of frontal circulation obviously is incomplete as fronts are influenced by time dependent processes which operate on timescales of the semi-diurnal tidal cycle and the fortnightly springs-neaps cycle as well as by episodic wind events. Within a tidal cycle, for example, tidal advection and straining of the density field by tidal current vertical shear are important processes. Over the springs-neaps cycle modulation of the level of tidal stirring causes periodic, non-linear advance and retreat of the mean frontal position, together with a general sharpening of the horizontal density gradients at springs (Simpson & Bowers 1981). Dynamical models

predict that both the frontal jet and frictionally induced transverse circulation will be enhanced at springs (Garrett & Loder 1981). Laboratory experiments of Linden & Simpson (1988) in a non-rotating system showed that baroclinic collapse of a horizontal density gradient is greatest when the level of ambient turbulence is low. These experiments thus suggest strongest cross-front circulation and sharpening of cross-front density gradients at neaps. Care should be taken, however, before these results are applied directly to rotating environments in which cross-front baroclinic relaxation will be transformed into along-front flow by geostrophic adjustment on an inertial timescale. Garrett & Loder (1981) showed that high turbulence levels enable energy to be extracted from the geostrophic jet and transferred to the cross-frontal circulation. This energy source is absent in the non-rotating case.

Episodic wind forcing can cause large-scale movement of front positions by increasing the available vertical mixing power (Simpson & Bowers 1981) and also, depending upon wind direction, by driving dense (mixed) water over lighter stratified water promoting convective instability (Wang *et al.* 1990). Cross-front circulation may be modified by increased levels of vertical mixing and by Ekman divergence across the frontal zone induced by wind forcing (Wang *et al.* 1990; Garrett & Loder 1981).

The above insights into frontal circulation are derived from one- or two-dimensional front models. Three-dimensional dynamical models such as those of James (1990) show that shelf sea fronts may be baroclinically unstable causing them to meander and shed eddies on the scale of the internal Rossby radius. These eddies have been reproduced in the laboratory by Griffiths & Linden (1982) and observed at fronts (Simpson & Pingree 1978).

The along-front jet is the component of frontal circulation which ought to be observed most readily but even this has proved elusive in observational studies such as that of Simpson *et al.* (1978). Probably the most convincing observations of a frontal jet are those of van Aken *et al.* (1987), who deployed current meter moorings in the vicinity of a front in the central North Sea for a duration of 38 days. During a three day period, as the front was advected past the mooring, a well-defined subsurface jet was observed with velocities up to $0.15\ \mathrm{m\ s^{-1}}$ which was in approximate geostrophic balance with the local density field. Although these observations are of high quality, they also serve to highlight the difficulty of keeping instruments in the dynamically active frontal zone for extended periods.

The availability of new instrument combinations has provided much of the technical capacity required to map currents synoptically in both horizontal and vertical planes, and hence there is renewed impetus to the effort of measuring frontal circulations. As part of the U.K. Natural Environment Research Council North Sea Project, studies were conducted between 1988 and 1989 to investigate the dynamics of a tidal mixing front in the North Sea.

2. Observational techniques

(*a*) *The study area*

Figure 2 shows the location of the North Sea frontal process studies. The front, shown schematically as a zig-zag line, separates vertically mixed water in the southern North Sea from water in the northern North Sea which is thermally stratified during spring and summer. Salinity is almost constant in the region. The front extends offshore from Flamborough Head on the English coast with a mean

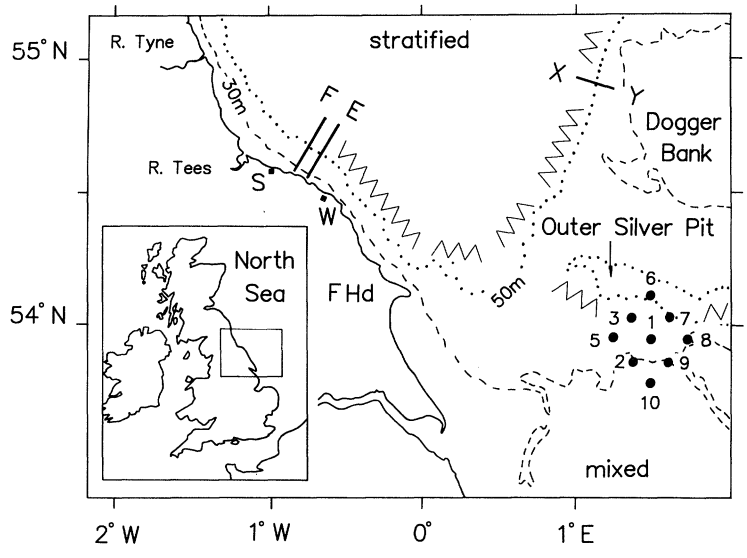

Figure 2. The North Sea fronts study area. Flamborough Head (F. Hd.), Saltburn (S) and Whitby (W). Solid circles indicate the release sites of Decca-Argos buoys.

position which corresponds with the h/u^3 criterion of Simpson & Hunter (1974). The front's existence was predicted on this basis by Pingree & Griffiths (1978). The front is predominantly a bottom feature but has a weak surface signature and is visible in satellite infrared images such as those shown in figure 3. The complete Flamborough frontal system consists of three distinct parts. North of Flamborough Head, the front is located about 10 km offshore and lies approximately parallel with the coast. From Flamborough Head, the front extends offshore and curls northward around the Dogger Bank (northern branch) with a southern branch situated over the deep Outer Silver Pit (figure 2). A model simulation of the density field described later (figure 9*c*) clarifies the relation between the various branches of the Flamborough frontal system. There is also evidence of significant interannual variability on the simplified pattern indicated in figure 2 (Gmitrowicz & Brown 1993).

Ship-borne observations were obtained in each of the three frontal regions during four cruises of the research vessel RRS *Challenger* in August 1988, September 1988, July 1989 and August 1989. Coincident with the August 1988 cruise, observations of the coastal part of the front were also made with a land-based radar system (OSCR).

In addition to conventional methods, combinations of the following techniques have been used to measure density and velocity fields in the frontal zone.

(*b*) *High frequency ocean surface current radar* (OSCR)

The HF radar is a unique oceanographic tool in providing a synoptic spatial mapping capability of surface currents averaged approximately over the top metre of the water column. The system utilizes Doppler shift by surface currents of Bragg-scattered radar returns from surface waves. One radar measures the component of velocity aligned radially from the radar site. Thus two transmitters are required to calculate vector velocities at beam intersections. The OSCR system operates at 27 MHz and enables surface currents to be measured up to 40 km offshore with current vectors which are spatial averages over cells of about 1 km^2 (Prandle & Matthews 1990). The location of the coastal part of the Flamborough front within

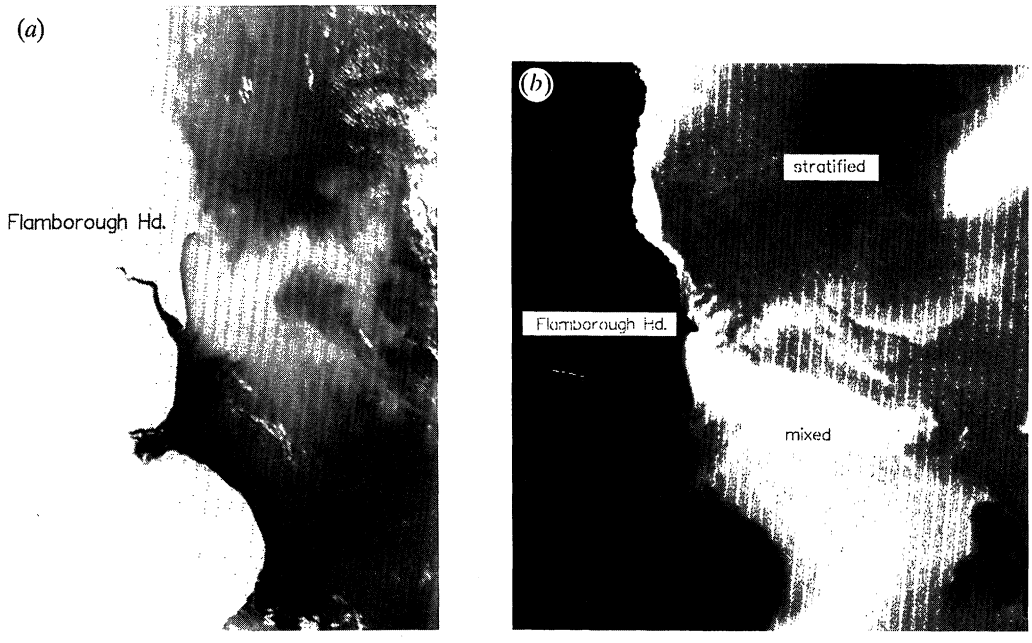

Figure 3. Satellite infrared images of the Flamborough frontal system, light areas indicate cold surface waters, dark areas represent warm surface water. (*a*) NOAA 11, 12 August 1991, 0310 GMT. The coastal front and both northern and southern branches of the offshore frontal system can be seen. (*b*) NOAA 9, 2 June 1985, 1327 GMT. Frontal instabilities with a wavelength and amplitude of about 10 km are visible as the front leaves the coast at Flamborough Head. These images were kindly provided by Dr P. Bayliss, Satellite Station, University of Dundee.

OSCR range thus provided an ideal opportunity for measurement of the surface circulation at a tidal mixing front. Two OSCR transmitters were simultaneously operated from 11 August to 3 September 1988 at two sites on the Yorkshire coast, Saltburn and Whitby (Matthews *et al.* 1993). Tides were extracted from OSCR records by harmonic analysis based on up to 30 tidal constituents and the wind-driven response of the surface current was removed using methods described by Prandle & Matthews (1990).

(*c*) *Ship-borne acoustic Doppler current profiler* (*ADCP*)

RRS *Challenger* was equipped with a 150 kHz hull-mounted ADCP. Operated in bottom-tracking mode, the ADCP is capable of measuring horizontal water velocity over the ground with an overall rms velocity uncertainty in the range 0.01–0.03 m s^{-1} depending upon averaging time and bin depth. The ADCP provided velocity estimates, in 4 m depth bins, below a surface shadow zone, 10 m deep, and above a bottom shadow zone which typically has a thickness of 15% of the total water depth. Details of the ADCP configurations used and a discussion of the estimated errors are given by Lwiza *et al.* (1991). The ADCP was used to obtain estimates of along and cross-front residual velocity fields on short sections across the front. The observational strategy was based on a technique first used by Simpson *et al.* (1990) to estimate the residual flow through a channel. The methods used to extract tides from these short data series are discussed by Simpson *et al.* (1990*b*) and Lwiza *et al.* (1991).

(d) *Towed, undulating* CTD (SEASOAR)

SEASOAR is a CTD system which is towed on an undulating flight-path behind the ship. In North Sea water depths, SEASOAR provides horizontal resolution equivalent to a conventional CTD cast approximately every 500 m. For the present studies the SEASOAR vehicle was equipped with a Neil Brown Mk III CTD. Although SEASOAR-type instruments have been available for some time (Allen *et al.* 1980), their use in combination with ship-borne ADCP enhances our measurement capability considerably by permitting the simultaneous high resolution mapping of both density and velocity fields which is ideal for frontal studies.

(e) *Decca-Argos drifting buoys*

Lagrangian methods of current measurement, such as free-drifting buoys, are an attractive alternative to conventional eulerian techniques in frontal zones because of the difficulty in maintaining moored instruments in a front for extended periods (Loder *et al.*, this symposium). The drifting buoys described here were designed specifically for the North Sea Project. Buoy design is described in detail by Roberts *et al.* (1991). Their novel feature is that they receive, and internally record every 10 min, position from the Decca hyperbolic radio navigation system which has coverage over the entire northwest European continental shelf. The dense time sampling gives rise to high spatial resolution drift tracks. Argos tracking enables buoy drift to be monitored during an experiment and greatly assists the recovery phase.

3. Results

(a) *Coastal front*

Figure 4 shows surface residual currents determined by HF radar after tides and wind response have been removed. These currents are interpreted as being largely density-driven flows (Matthews *et al.* 1993). Figure 4*a* shows the along-shore current component (central panel) and figure 4*b* the offshore component (central panel) for line E shown in figure 2. Figure 4 also shows along-shore geostrophic currents (figure 4*a*, top and bottom panels) which have been computed from the density sections shown in figure 4*b* (top and bottom panels) assuming zero velocity at the sea-bed. The two density sections were obtained on 21 August 1988 (neaps) and 29 August 1988 (springs).

Along-shore surface currents (figure 4*a*) were everywhere southeastwards along the coast (positive) consistent with flow measured by moored current meters during the experiment (Gmitrowicz & Brown 1993). For a day or so either side of spring tides on 29 August, the along-shore flow was intensified and was located in a position consistent with a geostrophic frontal jet. Cross-shore currents (figure 4*b*) gave the first experimental indication of surface convergence approximately 6.5 km from the coast during the spring-tide period centred on 29 August, coincident with the time when along-shore flow was most intense.

Although these results are suggestive of enhancement of both the frontal jet and frictionally-induced secondary circulation at spring-tides, aspects of the data do not concur with this interpretation. There is indication, for example, of slight along-shore flow enhancement at neaps and the density and geostrophic velocity sections exhibit little difference between the springs and neaps situations on 21 August and 29 August. There is also no evidence of along-shore flow intensification during the

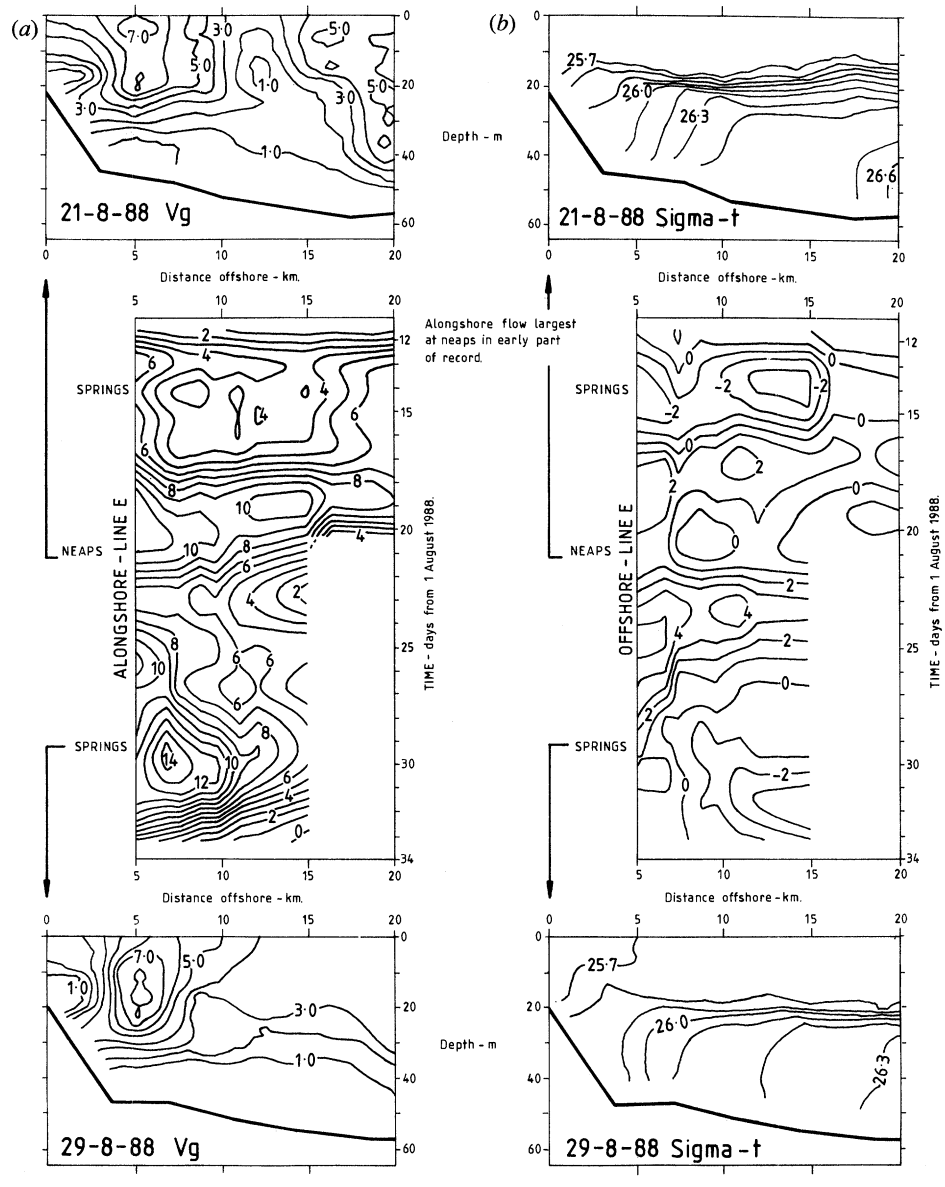

Figure 4. (*a*) Space-time plot of HF radar along-front surface currents (cm s^{-1}), normal to section E, (middle panel). Positive velocities are towards the south-east. Top and bottom panels show computed geostrophic currents (cm s^{-1}) relative to zero flow at the bed for the times indicated. (*b*) Cross-front currents (cm s^{-1}) parallel to section E (middle panel). Positive currents are directed offshore. Top and bottom panels show density, σ_t, sections for the time indicated.

first springs period, centred on 15 August, although there was onshore surface flow at that time. Matthews *et al.* (1993) have argued that the frontal jet and convergence could have been closer inshore during the first springs period and hence outside the coverage of the radar. Measured cross-shore surface currents were very weak (0.02 m s^{-1}), a value which is probably comparable with sources of error such as those arising from resolution into along-front and cross-front vector components,

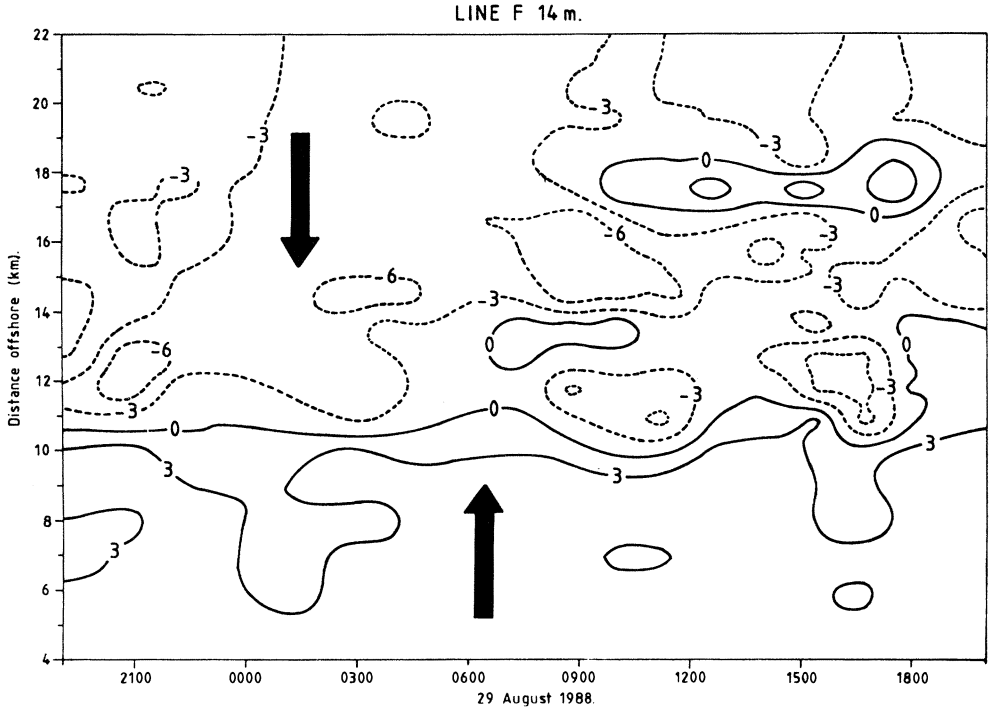

Figure 5. Space-time plot of ADCP residual velocities (cm s^{-1}) obtained on 28–29 August 1988 at a depth of 14 m on section F (figure 2). Positive velocities indicate offshore flow.

particularly if the front orientation was variable in time. It is surprising, however, that despite these possible errors, such a coherent space-time structure can be seen in the cross-shore current field.

Supporting evidence for the existence of surface flow convergence comes from cross-shore flows measured by ship-borne ADCP for a 25 h period on 29–30 August 1988 (Lwiza *et al.* 1991; Matthews *et al.* 1993) along the nearby F line. Figure 5 shows the cross-shore component of ADCP residual currents at a depth of 14 m and indicates convergence at about 10 km offshore. Equivalent ADCP residuals at mid-depth show no organized cross-shore flow pattern and near the bottom suggest flow divergence (Lwiza *et al.* 1991; Matthews *et al.* 1993).

(*b*) *Offshore fronts*

Figure 6 shows the density field, together with ADCP along-front residuals and computed geostrophic velocity obtained on 29 September 1988 from *XY* section (figure 2) across the northern branch of the Flamborough front near the Dogger Bank (Lwiza *et al.* 1991). Geostrophic velocities were computed relative to ADCP-derived residual velocities at 14 m depth. The observed frontal jet was less than 2 km wide with a maximum speed of about 0.15 m s^{-1} towards the northeast. The narrowness of the jet, together with temporal variability seen in the radar data, clearly demonstrates why it is so difficult to observe such features using conventional moored instrumentation. Other, indirect, evidence for flow along the northern branch of the front comes from CTD surveys in the region in September 1988 which showed a low salinity anomaly along the northern front consistent with advection of fresher, coastal water offshore (Smeed *et al.* 1993).

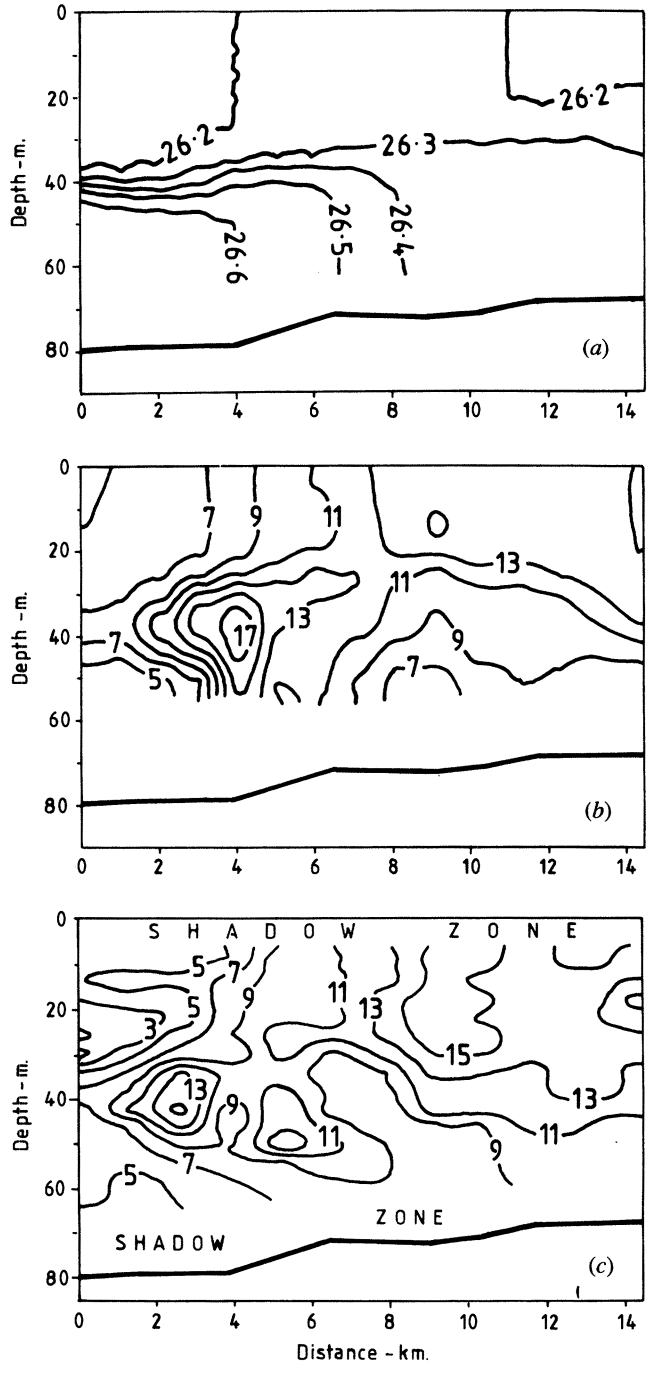

Figure 6. (*a*) Density, σ_t (*b*) geostrophic velocity (cm s^{-1}) relative to ADCP residual at 14 m depth (*c*) ADCP residual velocity obtained by least squares removal of tidal signal. Data obtained on *XY* section (figure 2) on 29 September 1988.

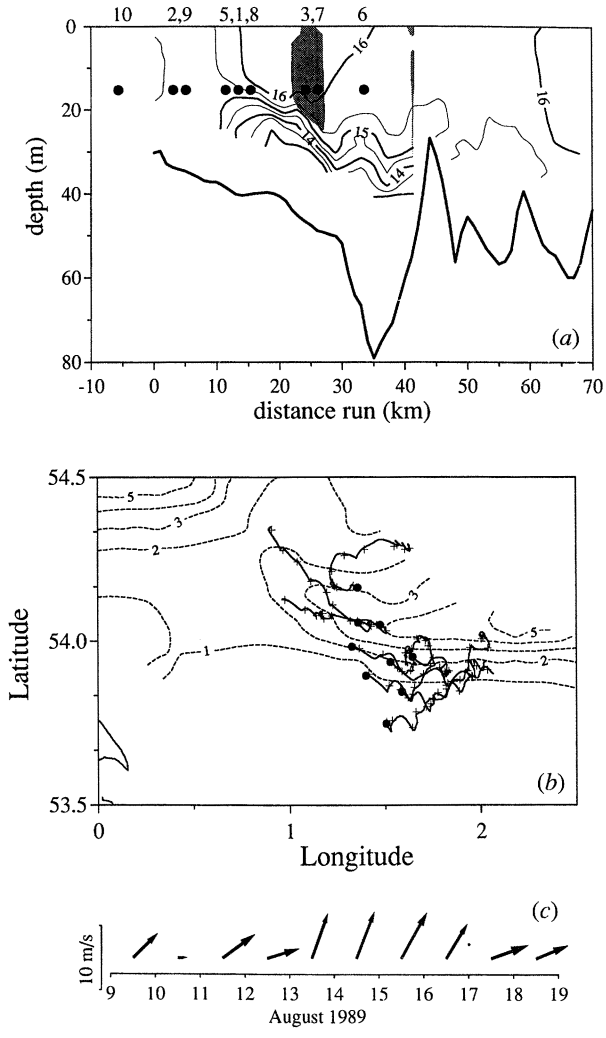

Figure 7. (*a*) North–south SEASOAR temperature (°C) section across the southern extension of the Flamborough front over the Outer Silver Pit at 1° 30′ E. Solid circles show the mean drogue depth of buoys deployed across the front on 9 August 1989. Buoy numbers are indicated at the top of the figure. The shaded region indicates where geostrophic velocity relative to the sea bed is greater than 0.08 m s^{-1} westwards. (*b*) Tidally filtered buoy trajectories for a 10 day duration, dashed lines show top to bottom temperature difference (°C) and (*c*) daily mean wind vectors from Spurn Point.

In August 1989 the southern branch of the Flamborough front, over the Outer Silver Pit, was seeded with nine Decca-Argos buoys, each drogued at a mean depth of 15 m below the sea surface with a 30 m^2 window blind drogue (Durazo *et al.* 1993). The locations of buoy deployments are shown in figure 2 and in figure 7*a*, which also shows a SEASOAR section through the deployment site. Three buoys (10, 2, 9) were laid on the mixed side of the front, three (5, 1, 8) were at the frontal transition and the remaining three (3, 7, 6) were on the stratified side. Figure 7*b* shows tidally filtered buoy trajectories and figure 7*c* shows daily mean wind vectors from Spurn Point (53° 40′ N, 0°). The apparent discrepancy in buoy start points between figures 2 and 7*b* arises because of data truncation due to tidal filtering. The trajectories show

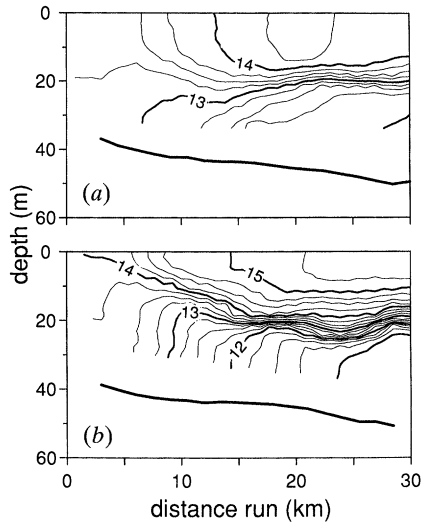

Figure 8. SEASOAR temperature (°C) sections across the southern branch of the Flamborough front along a north–south section at approximately longitude 1° 10′ E. (*a*) 15 July 1989 at 0029, 1.5 h before HW (after neaps). (*b*) 20 July 1989 at 0807, 1 h after HW (springs).

pronounced horizontal velocity shear across the front. The southern cluster of six buoys moved eastwards with a mean centre of mass speed of 0.034 m s^{-1}, while buoys 3 and 7 moved westwards with a mean centre of mass speed of 0.045 m s^{-1}. The northern-most buoy (6) moved initially westwards before turning eastwards. The southern buoy cluster was probably influenced by wind-driven flow, but buoys north of the front clearly moved independently of the wind direction in a direction consistent with geostrophic flow (figure 7*a*).

Lwiza (1990) examined ADCP sections, obtained in the offshore front system but, unlike the coastal front, found no direct evidence of systematic patterns of cross-front circulation. SEASOAR sections obtained at the southern front in July and August 1989 exhibited considerable variability both within a tidal cycle, due to straining, and over a springs-neaps period. Figure 8 shows sections obtained at approximately the same state of the tide (within 1 h of high water) just after neaps and at springs in July 1989. Upwelling of cold bottom water on the mixed side of the surface front at springs is suggested by the upward-doming of the 13 °C isotherm (figure 8*b*). Another feature of the numerous high resolution SEASOAR sections obtained, but not shown here, is that in many cases there is 'multi-frontal' structure with a number of regions of large horizontal gradient separated by areas of weaker gradients (Smeed *et al.* 1993).

(*c*) *Dispersion and mixing near the front*

Durazo *et al.* (1993) have estimated horizontal eddy diffusivities, K_A and K_C, for along-front and cross-front directions using the single-particle statistics of Decca-Argos buoy trajectories. Both K_A and K_C were about 80 m^2 s^{-1} for the southern cluster of six buoys. The implied lagrangian (eddy) length scale was about 1 km for both along-front and cross-front directions with an integral timescale of 5–9 h.

The simultaneous use of SEASOAR and ADCP has permitted direct estimates of the gradient Richardson number, *Ri*, to be obtained in the upper part of the water

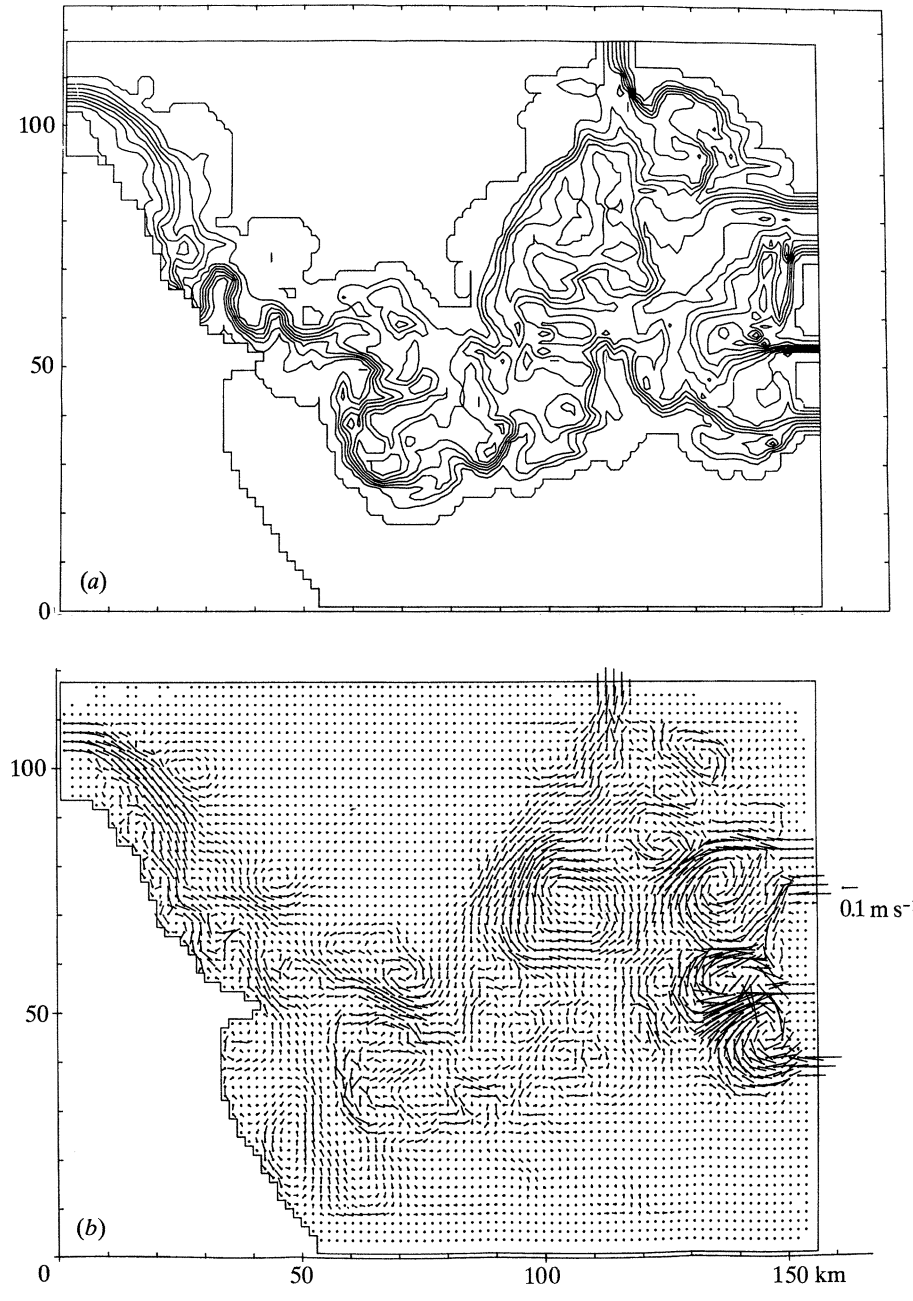

Figure 9. Results from a numerical model of the density-driven circulation in the Flamborough front. (*a*) Surface density contours and (*b*) surface currents for a frictionless run.

column. These show that vertical mixing occurred in regions of low *Ri* caused by a strong wind event (Smeed *et al.* 1993).

(*d*) *Eddies and instabilities*

Satellite infrared images of the Flamborough frontal region occasionally show eddies and instabilities. Figure 3*b* shows a particularly dramatic example where large

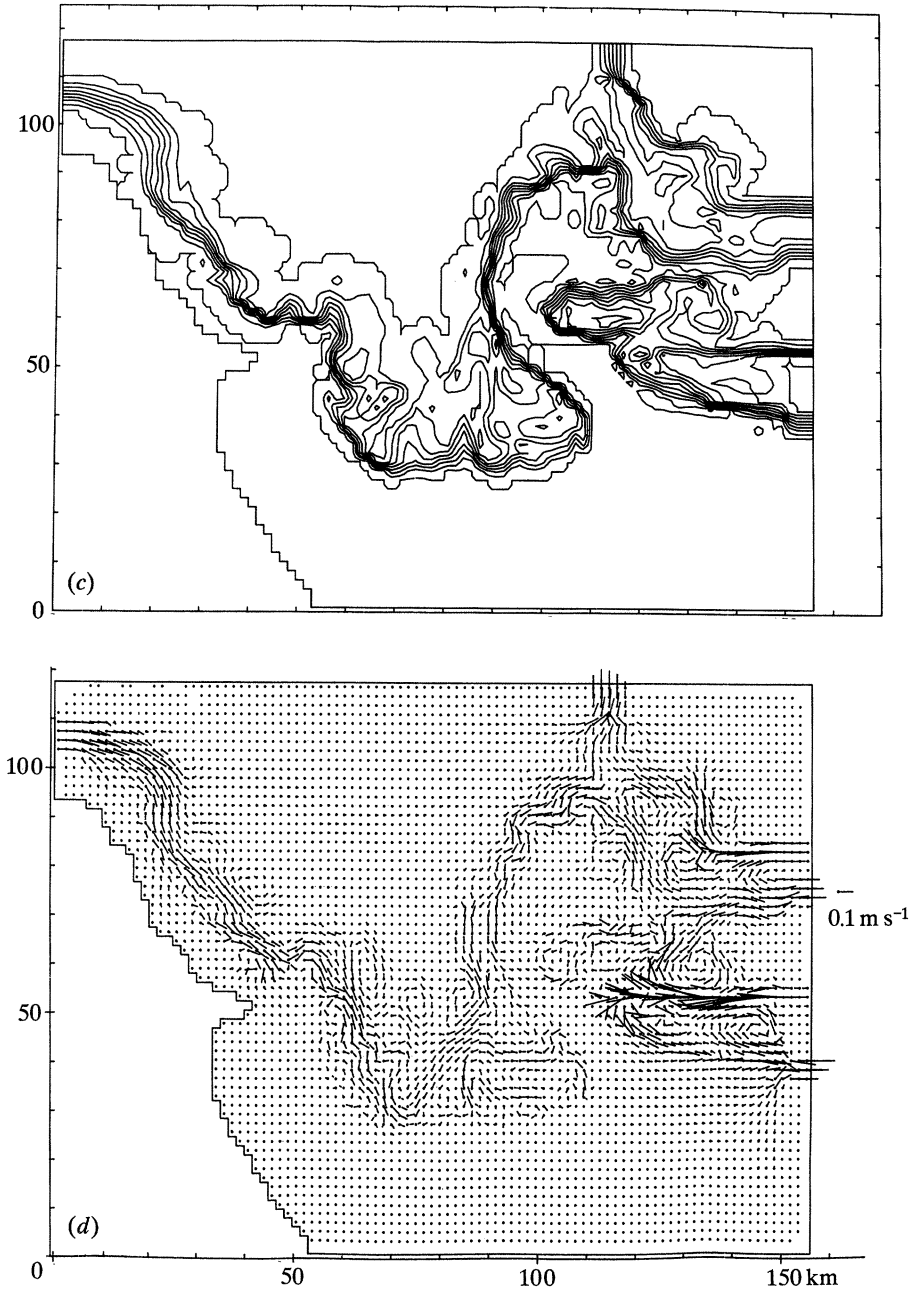

Figure 9. (*c*) Surface density contours and (*d*) surface currents with friction and vertical mixing included.

meanders of order 10 km wavelength are present at the front, apparently as a result of instability as the front leaves the coast (Fox 1989). This length scale is consistent with that expected as the Rossby deformation radius is about 4 km.

Little direct evidence of coherent structures that might be associated with frontally generated baroclinic eddies was found during the study. Indeed, in the case

of the coastal front, the coherence of along and cross shore flows strongly suggested that eddies were absent. Parallel SEASOAR sections, closely spaced in the along-front direction, however, showed large curvature of the northern bottom front consistent with the expected scale of frontal eddies (Smeed *et al.* 1993).

James (1989, 1990) has used a three-dimensional, eddy-resolving, numerical model based upon primitive equations and capable of evolving the density field to investigate the Flamborough frontal system. The model covers both the coastal and offshore frontal regions with a grid spacing of 1.6×1.8 km^2. The model was run using realistic bathymetry and initial density and geostrophic velocity conditions based upon observed stratification.

Figure 9*a* shows surface density contours, after six model days, in a run for which bottom friction and vertical mixing are absent. Large instabilities are visible near Flamborough Head which bear a remarkable resemblance to the satellite image in figure 3*b*. The modelled currents (figure 9*b*) reveal cyclonic eddies offshore from the coastal front with spacing of about 25 km. As shown by the convoluted density field, these eddies exist within the stratified region and do not have a significant effect on surface or bottom fronts. When vertical mixing (vertical eddy viscosity and eddy diffusivity up to 200 cm^2 s^{-1} in mixed water and beneath the thermocline) and bottom friction, arising from a mean square tidal velocity of 0.125 m^2 s^{-2}, are included much of the instability is damped out, as shown in figure 9*c*, again after six model days. The meandering of the flow off Flamborough Head may thus be conditional on low friction conditions which may occur only during neap tides. An examination of all available infrared images in relation to time in the springs-neaps cycle may cast light on this question. Bathymetry plays an important role in stabilising the flow because frictionless model runs using a flat bottom but the same initial conditions result in very large frontal instabilities. The combined effects of the proximity of the coast and frictional effects thus stabilise the flow and prevent the development of eddy instability in the coastal front making it possible to detect the rather weak transverse circulation due to frictional effects in a two-dimensional front.

4. Discussion

The role of the Flamborough front in the North Sea system remains uncertain. The main question is whether it acts as a barrier inhibiting summer-time transport of passive contaminants between the northern and southern North Sea. In the absence of eddies, the front is probably best viewed as a barrier to dispersion and this régime may best describe the coastal front zone. The lack of evidence for eddies in offshore regions of the Flamborough front is not conclusive, however, given the relatively limited spatial sampling. Baroclinic eddies generated at fronts such as those appearing in the model simulations of James (1989, 1990), would help to promote cross-frontal mixing.

The circulation pattern we have observed is consistent with the view that passive contaminants introduced into the North Sea coastal zone, via estuaries such as the Tyne and the Tees on the northeast coast of England, will be transported south-eastwards along the coast. We have obtained evidence, however, that density-driven flows associated with the coastal front constitute an important component of this transport. The density-driven flow apparently coexists with energetic, intermittent wind-driven inertial flows suggesting that linear superposition of these flow components may be appropriate. Our observations also suggest that the frontal jet

will transport contaminants offshore at Flamborough Head, into the northern front. In contrast, however, there is indication of onshore transport on the stratified side of the southern front. The pronounced horizontal shear across the southern front indicates that shear diffusion may be important in spreading contaminant offshore along that part of the frontal zone.

The North Sea Project has provided some of the first direct measurements of circulations driven by shelf sea frontal density gradients. These observations, together with other recent front studies (Hill *et al.* 1993; Loder *et al.*, this symposium), have been made possible by the use of a range of novel techniques which involve rapid, quasi-synoptic sampling in the frontal zone. In this respect these efforts represent the genesis of a new approach to the observation of frontal dynamics. The new generation of eddy resolving frontal circulation models (James 1989, 1990) promise to assist greatly the planning of future fronts dynamics experiments.

The total length of the frontal interface between tidally mixed and summer-stratified water on the northwest European continental shelf is at least 1500 km. Along the length of these fronts important dynamical processes take place which influence nutrient availability for primary production and the transport of passive contaminants. The new range of observational techniques, demonstrated for the first time in the North Sea Project, has already given rise to a modest advance in our perception of these processes, and has laid the foundation for making the necessary dynamical observations that will enable the details of these processes to be measured and eventually modelled.

References

van Aken, H. M., Van Heijst, G. J. F. & Maas, L. R. M. 1987 Observation of fronts in the North Sea. *J. mar. Res.* **45**, 579–600.

Allen, C. M., Simpson, J. H. & Carson, R. M. 1980 The structure and variability of shelf sea fronts observed by an undulating CTD system. *Oceanologica Acta* **3**, 59–68.

Durazo, R., Hill, A. E., Smeed, D. A. & Linden, P. F. 1993 Horizontal circulation and dispersion estimates at a tidal mixing front in the North Sea. *Cont. Shelf Res.* (Submitted.)

Fox, A. D. 1989 Satellite infra-red observations of instabilities on the Flamborough Head front. M.Sc. thesis, University of Wales, Bangor.

Garrett, C. J. R. & Loder, J. W. 1981 Dynamical aspects of shallow sea fronts. *Phil. Trans. R. Soc. Lond.* A **302**, 563–581.

Gmitrowicz, E. M. & Brown, J. 1993 The variability and forcing of currents within a frontal region off the north-east coast of England. *Cont. Shelf Res.* (In the press.)

Griffiths, R. W. & Linden, P. F. 1982 Laboratory experiments on fronts. Part 1: density driven boundary currents. *Geophys. Astrophys. Fluid Dynamics* **19**, 159–187.

Hill, A. E., Durazo, R. & Smeed, D. A. 1993 Observations of a cyclonic gyre in the western Irish Sea. *Cont. Shelf Res.* (In the press.)

James, I. D. 1978 A note on the circulation induced by a shallow sea front. *Est. Coast. mar. Sci.* **7**, 197–202.

James, I. D. 1989 A three-dimensional model of circulation in a frontal region in the North Sea. *Dt. hydrogr. Z.* **42**, 231–247.

James, I. D. 1990 Numerical modelling of density-driven circulation in shelf seas. In *Modelling marine systems*, vol. II (ed. A. M. Davies), pp. 345–372. Boca Raton, Florida: CRC Press.

Le Fèvre, J. 1986 Aspects of the biology of frontal systems. *Adv. mar. Biol.* **23**, 164–299.

Linden, P. F. & Simpson, J. E. 1988 Modulated mixing and frontogenesis in shallow seas and estuaries. *Cont. Shelf Res.* **8**, 1107–1127.

Lwiza, K. M. M. 1990 A study of tidal front dynamics using acoustic Doppler current profiler. Ph.D. thesis, University of Wales, Bangor.

Lwiza, K. M. M., Bowers, D. G. & Simpson, J. H. 1991 Residual and tidal flow at a tidal mixing front in the North Sea. *Cont. Shelf Res.* **11**, 1379–1395.

Matthews, J. P., Fox, A. & Prandle, D. 1993 Radar observation of an along-front jet and transverse convergence associated with a North Sea front. *Cont. Shelf Res.* **13**, 109–130.

Pingree, R. D. & Griffiths, D. K. 1978 Tidal fronts on the shelf seas around the British Isles. *J. Geophys. Res.* **83**, 4615–4622.

Prandle, D. & Matthews, J. P. 1990 The dynamics of nearshore surface currents generated by tides, wind and horizontal density gradients. *Cont. Shelf Res.* **10**, 665–681.

Roberts, G., Last, J. D., Roberts, E. W. & Hill, A. E. 1991 Position-logging drifting buoys using Decca navigator and Argos for high-resolution spatial sampling. *J. atmos. oceanic Technol.* **8**, 718–728.

Simpson, J. H. 1981 The shelf sea fronts: implications of their existence and behaviour. *Phil. Trans. R. Soc. Lond.* A **302**, 531–536.

Simpson, J. H. & Hunter, J. R. 1974 Fronts in the Irish Sea. *Nature, Lond.* **250**, 404–406.

Simpson, J. H. & Pingree, R. D. 1978 Shallow sea fronts produced by tidal stirring. In *Oceanic fronts in coastal processes* (ed. M. J. Bowman & W. E. Esaias), pp. 29–42. New York: Springer-Verlag.

Simpson, J. H., Allen, C. M. & Morris, N. C. G. 1978 Fronts on the continental shelf. *J. geophys. Res.* **83**, 4607–4614.

Simpson, J. H. & Bowers, D. G. 1981 Models of stratification and frontal movement in shelf seas. *Deep Sea Res.* A **28**, 727–738.

Simpson, J. H., Mitchelson-Jacob, E. G. & Hill, A. E. 1990 Flow structure in a channel from an acoustic Doppler current profiler. *Cont. Shelf Res.* **10**, 589–603.

Smeed, D. A., Linden, P. F. & Hill, A. E. 1993 Observations of North Sea fronts. *Cont. Shelf Res.* (Submitted.)

Soulsby, R. L. 1983 The bottom boundary layer of shelf seas. In *Physical oceanography of coastal and shelf seas* (ed. B. Johns). Amsterdam: Elsevier.

Wang, D.-P., Chen, D. & Sherwin, T. J. 1990 Coupling between mixing and advection in a shallow sea front. *Cont. Shelf. Res.* **10**, 123–136.

Discussion

M. Weydert. What is the accuracy of the tidal filtering used in deriving residual currents in the vicinity of the front?

D. Prandle. A particular feature of the results presented was the careful use of filtering techniques. The papers by Prandle & Matthews (1990) and by Matthews *et al.* (1993) show how such techniques enabled separate flow components involving inertial, frontal and monthly averaged density driven currents to be isolated.